

1 **Talin and Vinculin are Downregulated in Atherosclerotic Plaque; Tampere Vascular Study**

2 Magdaléna von Essen^{1*}, Rolle Rahikainen^{1*}, Niku Oksala^{2,3}, Emma Raitoharju², Ilkka Seppälä², Ari
3 Mennander⁴, Thanos Sioris⁴, Ivana Kholova⁵, Norman Klopp⁶, Thomas Illig^{6,7,8}, Pekka Karhunen⁹, Mika
4 Kähönen¹⁰, Terho Lehtimäki^{2†}, Vesa P. Hytönen^{1†}

5
6
7 ¹ BioMediTech, University of Tampere and Fimlab Laboratories, Tampere, Finland

8 ² Dep. of Clinical Chemistry, Fimlab Laboratories, Tampere University Hospital and School of
9 Medicine, University of Tampere, Tampere, Finland

10 ³ Division of Vascular Surgery, Department of Surgery, Tampere University Hospital, Tampere,
11 Finland

12 ⁴ Heart Center, Tampere University Hospital, Tampere, Finland

13 ⁵ Department of Pathology, Fimlab Laboratories, Tampere University Hospital and School of Medicine,
14 University of Tampere, Tampere, Finland

15 ⁶ Hannover Unified Biobank, Hannover Medical School, Hannover, Germany.

16 ⁷ Institute of Human Genetics, Hannover Medical School, Hannover, Germany.

17 ⁸ Research Unit of Molecular Epidemiology, Helmholtz Zentrum München, German Research Center
18 for Environmental Health, Neuherberg, Germany.

19 ⁹ School of Medicine, University of Tampere and Fimlab Laboratories, Tampere University Hospital,
20 Tampere, Finland

21 ¹⁰ Department of Clinical Physiology, Tampere University Hospital and School of Medicine, University
22 of Tampere, Tampere, Finland.

23

24 * , † These authors contributed equally to this work

25

26 Short Title: Talin and Vinculin in human atherosclerosis

27

28 Corresponding author:

29 Vesa Hytönen

30 BioMediTech,

31 Lääkärintätkatu 1, FI-33520 Tampere, Finland

32 email: vesa.hytonen@uta.fi

33 Phone: +358401901517

34

35 **Abstract**

36 Background. Focal adhesions (FA) play an important role in the tissue remodeling and in the
37 maintenance of tissue integrity and homeostasis. Talin and vinculin proteins are among the major
38 constituents of FAs contributing to cellular well-being and intercellular communication.

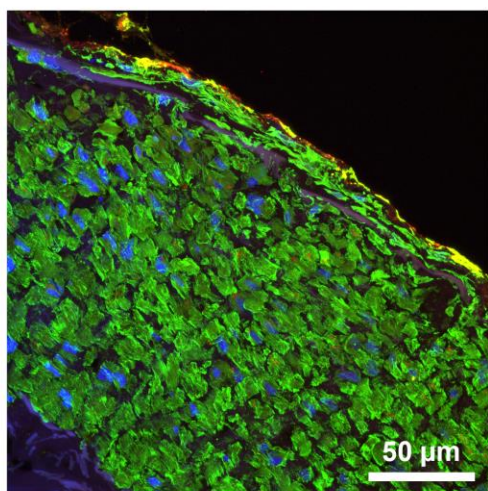
39 Methods and Results. Microarray analysis (MA) and qRT-PCR low-density array were implemented to
40 analyze talin-1, talin-2, meta-vinculin and vinculin gene expression in circulating blood and arterial
41 plaque. All analyzed genes were significantly and consistently downregulated in plaques (carotid,
42 abdominal aortic and femoral regions) compared to left internal thoracic artery (LITA) control. The use
43 of LITA samples as controls for arterial plaque samples was validated using immunohistochemistry by
44 comparing LITA samples with healthy arterial samples from a cadaver. Even though the differences in
45 expression levels between stable and unstable plaques were not statistically significant, we observed
46 further negative tendency in the expression in unstable atherosclerotic plaques. The confocal tissue
47 imaging revealed gradient of talin-1 expression in plaque with reduction close to the vessel lumen.
48 Similar gradient was observed for talin-2 expression in LITA controls but was not detected in plaques.
49 This suggests that impaired tissue mechanostability affects the tissue remodeling and healing
50 capabilities leading to development of unstable plaques.

51 Conclusion. The central role of talin and vinculin in cell adhesions suggests that the disintegration of
52 the tissue in atherosclerosis could be partially driven by downregulation of these genes, leading to
53 loosening of cell-ECM interactions and remodeling of the tissue.

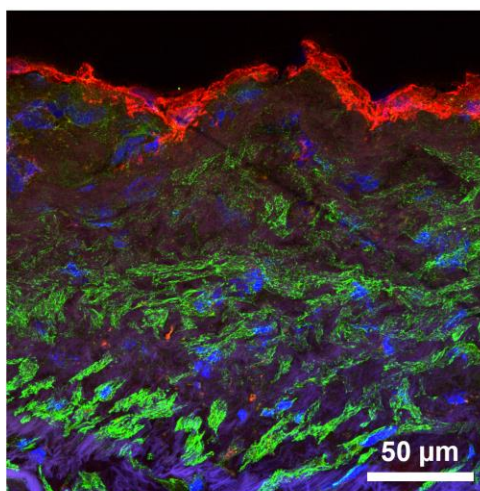
54

55 **Graphical abstract**

LITA



Plaque



Talin-1

PECAM-1

DAPI

56

57

58 **Highlights**

- 59 1. Talin and vinculin are downregulated in atherosclerotic plaques in all arterial beds
60 2. Expression of talin-1 in plaque is severely downregulated close to vessel lumen
61 3. Talin-2 expression in LITA shows a gradient towards vessel lumen which is absent in the
62 plaque
63 4. The talin and vinculin expression may be further reduced in with progression of the disease,
64 i.e. in later stages of plaque development and thrombosis
65 5. Talin and vinculin downregulation in atherosclerotic plaque causes tissue disorganization and
66 may lead to reduced tolerance against mechanical impacts and impaired healing processes

67

68 **Keywords**

69 Mechanobiology, atherosclerosis, focal adhesion, talin, vinculin

70

71 **Abbreviations**

BMI	-	Body Mass Index
CAD	-	Coronary Artery Disease
ECM	-	Extracellular matter
FA	-	Focal Adhesion
FC	-	Focal Complex
fc	-	fold change
HUVEC	-	Human Umbilical Vein Endothelial Cell
ICAM	-	Intercellular Adhesion Molecule
LDA	-	Low Density Array
LITA	-	left internal thoracic artery
MA	-	Microarray Analysis
MΦ	-	Macrophage
PECAM	-	Platelet endothelial cell Adhesion Molecule
SMC	-	Smooth Muscle Cell
TVS	-	Tampere Vascular Study
VBS	-	Vinculin Binding Site
VCAM	-	Vascular Cell Adhesion Molecule
FFPE	-	Formalin-Fixed, Paraffin-Embedded
HE	-	Hematoxylin-Eosin

72

73 Introduction

74 Atherosclerosis is a disease of the vasculature with a complex etiology. Risk factors include age, sex,
75 family history, dyslipidemia, high blood pressure and high body mass index (BMI), stress and dietary
76 factors. The disease develops over a long time period and may remain asymptomatic over decades. It
77 is characterized by chronic inflammation of the arterial wall, by infiltration of macrophages (M Φ) and
78 accumulation of oxidized low-density lipoproteins leading to M Φ conversion to foam cells [1].

79 The vasculature is continuously exposed to cyclical fluctuations of blood flow, pressure and fluid shear
80 stress and also exhibits diurnal variation. The blood mechanical impacts of varying magnitudes exert
81 significant influences on physiological and pathophysiological processes [2] [3] [4]. For illustration,
82 veins and arteries are composed of several tissue layers with different cell and extra-cellular matter
83 (ECM) content. This cell and ECM composition determines the tissue characteristics in terms of
84 physicochemical properties [5] [6]. Hence, each vessel layer possesses different ability to withstand,
85 produce or transduce mechanical forces [5]. The mechanical pressure sensed by the endothelial cells
86 is transferred from the extracellular space through the actin cytoskeletal network towards the nucleus
87 [7] [8].

88 To date, a number of genes implicated in cellular mechanostability and their altered expression has
89 been associated with the progress of atherosclerosis. For example, ADAM metalloprotease
90 disintegrins have been linked with cell-cell/surface adhesion and inflammation progression in the
91 atherosclerotic plaque [9]. Moreover, the expression levels of integrin and kindlin family proteins were
92 found to be altered in progressing atherosclerotic plaques [10]. Integrin and kindlin proteins support
93 leukocyte adhesion, transendothelial migration, platelet aggregation and thrombosis. Furthermore,
94 integrins and kindlins are together with talin and vinculin among the major components of focal
95 adhesions (FA). FAs are key attachments between cells and ECM and play an important role in cell
96 morphology, differentiation, locomotion and intercellular communication. FAs are crucial for the tissue
97 remodeling, integrity and homeostasis through the maintenance of intercellular gaps and cell adhesion
98 supervision.

99 Talin is a large flexible protein [11] binding to transmembrane integrins (N-terminal FERM domain) [12]
100 and to cytoskeletal actin (C-terminal rod) [13] providing a vital link between the intra- and extracellular
101 space and allowing the communication between the ECM and nucleus [8]. Talin plays a significant role
102 in the actin filament assembly and in spreading and migration of various cell types. During the
103 adhesion maturation, talin recruits vinculin to crosslink with F-actin filaments and stabilize the
104 adhesion complex. For this purpose talin rod contains several binding sites for vinculin [14]. Vinculin
105 binding sites (VBSs) are buried inside the structural bundles and require a major conformational
106 change in the bundle organization prior to vinculin binding [15]. Mechanical force has been suspected
107 to mediate such domain reorganization and talin-vinculin binding [16] [17]. Talin interacts with several
108 ligands making it a vital component of numerous mechanosensor and chemical signaling pathways
109 [18] [19] [20] [21].

110 Vinculin is a cytoskeletal protein crosslinking talin and F-actin. Vinculin is ubiquitously expressed with
111 high expression in skeletal, cardiac and smooth muscle. Vinculin head at the N-terminal end binds to
112 talin's VBSs [22]. Vinculin tail at the C-terminal end binds F-actin [23]. Also other important
113 interactions of vinculin have been recognized, for example with paxilin [24] and α -actinin [25]. These
114 ligands make vinculin an important contributor to focal adhesion complex, as well as to the
115 cytoskeletal assembly and stability.

116 The progress and the causatives of atherosclerosis have been intensively investigated during the past
117 decades. Still, the mechanisms behind the disease development are not fully understood. In more
118 detail, the mechanical impact of shear stress on the cell and tissue integrity has risen to attention only
119 recently. We hypothesize that the cellular mechanostability and maintenance of tissue integrity
120 through focal adhesions is an important factor in all stages of atherosclerotic plaque development. We

121 speculate that the function of focal adhesions is compromised by altered expression of cell adhesion
122 proteins talin and vinculin in atherosclerotic plaque as compared to non-atherosclerotic vessel wall.

123 In this work we followed talin and vinculin expression in atherosclerotic plaque samples collected in
124 ongoing Tampere Vascular Study (TVS) series. Gene expression in carotid, abdominal aortic and
125 femoral plaque samples was compared to expression values in left internal thoracic artery (LITA)
126 controls. Expression levels were determined by microarray analysis and low-density qRT-PCR-array.
127 Results are supported by smooth muscle cell (SMC) and macrophage (MΦ) marker co-expression
128 analysis. The tissue localization of talin and vinculin was investigated by confocal immunofluorescence
129 study.

130

131 **Methods**

132 **Vascular Samples**

133 Arterial sample series from Tampere Vascular Study (TVS) [9] [26] [10] including samples from
134 femoral, carotid and abdominal aortic regions were obtained during open vascular procedures
135 between 2005 and 2015. The patients fulfilled the following inclusion criteria: (1) carotid
136 endarterectomy performed because of asymptomatic or symptomatic and hemodynamically significant
137 carotid stenosis (>70%); (2) femoral or (3) aortic endarterectomy with aortoiliac or aortobifemoral
138 bypass based on symptomatic peripheral arterial disease. The left internal thoracic artery (LITA)
139 controls were obtained during coronary artery bypass surgery due to coronary artery disease (CAD).
140 The samples were collected from patients subjected to open vascular surgery in the Division of
141 Vascular Surgery and Heart Center, Tampere University Hospital. The patient's denial to participate in
142 the study was used as a measure of exclusion. The vascular samples were classified according to
143 American Heart Association recommendation [27]. The type V and VI atherosclerotic lesions were
144 further histologically classified as stable and unstable according to the presence of fissure, rupture,
145 hemorrhage or thrombosis. Gene expression was analyzed from carotid (n=29), abdominal aortic
146 (n=15), and femoral (n=24) plaques (*cases*) and compared to atherosclerosis-free LITA samples
147 (n=28) (*controls*). The study has been approved by the Ethics Committee of Tampere Hospital District.
148 All studies were conducted according to the declaration of Helsinki, with the informed consent from
149 individual patient involved.

150 **Whole Blood and Circulating Monocyte Fractions**

151 TVS whole blood and monocyte fractions were collected during 2008. The angiographically verified
152 samples were selected from a larger population-based cross-sectional study [28] collected between
153 2001 and 2004 comprising patients subjected to an exercise test at Tampere University Hospital
154 (treatment according to the Finnish Current Care Guidelines). RNA was isolated from the whole blood
155 and monocyte fractions of individuals with CAD (n=55) and without coronary artery lesions (n=45).
156 Patient history data were based on hospital records and patient interviews. These data covered the
157 demographics such as age, sex, weight, lifestyle information and classical cardiovascular risk factors
158 and symptoms.

159 **RNA Isolation and Microarrays**

160 The fresh arterial tissue samples were soaked in RNALater solution (Ambion Inc, Austin, TX) and
161 isolated with Trizol reagent (Invitrogen, Carlsbad, CA) and the RNeasy Kit with DNase Set (Qiagen,
162 Valencia, CA). From the whole blood fraction, the RNA was isolated with PAXgene tubes (BD,
163 Franklin Lakes, NJ) and PAXgene Blood RNA Kit (Qiagen) with DNase Set. Peripheral mononuclear
164 cells were isolated from the whole blood samples by Ficoll-Paque density-gradient centrifugation
165 (Amersham Pharmacia Biotech UK Limited, Buckinghamshire, England). Total RNA was then
166 extracted using RNeasy Mini Kit (Qiagen). Manufacturers' instructions were followed in all isolation
167 protocols. The quality of the RNA samples was evaluated spectrophotometrically and stored at -80°C.

168 The expression levels of arterial and whole blood samples were analyzed with Illumina HumanHT-12
169 v3 Expression BeadChip (Illumina, San Diego, CA) analyzing 47 000 transcripts of all known genes,
170 gene candidates, and splice variants. The microarray experiments for the monocyte RNA were
171 performed using Sentrix Human-6 Expression BeadChips analyzing >46 000 transcripts (Illumina).
172 Both arrays were run according to given instructions by the manufacturer and scanned with the
173 Illumina iScan system. Further details of the methodology can be found in work by Turpeinen et al.
174 [29].

175 **Microarray Data Analysis**

176 After background subtraction, raw intensity data were exported using the Illumina GenomeStudio
177 software. Raw expression data were imported into R software, log₂ transformed and normalized by
178 the locally estimated scatterplot smoothing normalization method implemented in the R/Bioconductor
179 package Lumi. Locally estimated scatterplot smoothing normalization returned the best accuracy to
180 detect differentially expressed genes in comparison with quantitative reverse transcription polymerase
181 chain reaction using the control artery (LITA) and atherosclerotic plaque samples from the TVS study
182 [30]. All samples fulfilled following data quality control criteria; detection of outlier arrays based on the
183 low number of robustly expressed genes and hierarchical clustering. Probes were considered robustly
184 expressed if the detection was $p < 0.05$ for minimum of 50% of the samples in the data set. *TLN1*
185 (microarray element probe ILMN_1696643), *TLN2* (microarray element probe ILMN_1700042) and
186 *VCL* (transcript variant 1, microarray element probe ILMN_1795429; transcript variant 2, microarray
187 element probe ILMN_2413527) genes were selected for differential expression and correlation
188 analyses. These results were further confirmed by low-density qRT-PCR array.

189 **Low-density qRT-PCR-array (LDA)**

190 The quantitative real-time polymerase chain reaction (qRT-PCR) was performed with TaqMan low-
191 density array (LDAs; Applied Biosystems) according to the manufacturer's instructions. The
192 functionality of TaqMan assays, the optimal amounts of RNA in cDNA synthesis and optimal amount
193 of cDNA in qRT-PCR were first optimized for functional range and validated for inhibition using several
194 concentrations in separate TaqMan assays. Sufficient RNA was available for 19 out of 24 LITAs
195 (79.2%) and 64 out of 68 plaque (94.2%) samples. 60 (30 cases and 30 controls) out of 96 blood
196 samples (62.5%) were selected for analysis based on pairwise matching according to BMI, age,
197 gender and smoking status. In detail, 500 ng of total RNA per sample was transcribed to cDNA using
198 the High Capacity cDNA Kit (Applied Biosystems). For the qPCR, LDAs were loaded with 7 μ l cDNA
199 synthesis product (175 ng of RNA), 43 μ l H₂O and 50 μ l PCR Universal Master Mix (Applied
200 Biosystems). The array contained technical triplicates. Glyceraldehyde-3-phosphate dehydrogenase
201 (GAPDH, assayID Hs99999905_m1) was used as housekeeping gene control. The qRT-PCR data
202 was analyzed with Expression suite software (Applied biosystems) using the 2- $\Delta\Delta$ CT method.

203 **Hierarchical Clustering and Correlation Analyses**

204 *TLN1*, *TLN2*, *VCL* and well-characterized biomarkers of inflammation (cluster of differentiation 68
205 (CD68) and arachidonate 5-lipoxygenase (ALOX5)), and SMCs markers (calponin 1 (CNN1),
206 smoothelin (SMTN)) [31] were used in the hierarchical clustering analysis to assess whether
207 subgroups of samples had similar marker profiles. Furthermore, similarity of the expression levels
208 (*TLN1*, *TLN2* and *VCL*) across the samples was studied. The procedure was performed using the
209 heatmap.2 function from the gplots R library on all 68 artery samples. Pearson dissimilarity and
210 average linkage were used for the hierarchical clustering of both genes and samples. To further
211 investigate the *TLN1*, *TLN2* and *VCL* genes as measures of plaque cell composition, correlation
212 analyses were performed using previously established macrophage and SMC-rich plaque signatures
213 [31].

214

215 **Confocal Immunofluorescence Study of Frozen and Paraffin-Embedded Samples**

216 For immunofluorescence labeling of frozen tissue sections, vascular samples from LITA and from
217 atherosclerotic carotid artery were embedded into TissueTek O.C.T compound (Sakura Finetek, USA),
218 frozen in liquid nitrogen and stored at -80°C . Leica CM 3050S (Leica Biosystems, Nussloch,
219 Germany) cryostat was used to cut $6\ \mu\text{m}$ sections of the frozen tissues. Before antibody staining, the
220 tissue sections were air-dried at room temperature for 20 minutes and fixed with acetone at -20°C for
221 10 minutes. Fixed samples were air-dried for 15 minutes at room temperature, immersed into PBS
222 (pH 7.4) and transferred to Shandon Sequenza (Thermo Shandon Ltd, Runcorn, UK) immunostaining
223 cassettes. Nonspecific antibody binding was blocked by preincubating the tissue sections in blocking
224 buffer containing 1% BSA and 0.3% Triton-X100 diluted in PBS (pH 7.4). All antibodies were diluted
225 into the blocking buffer. The following primary antibodies were used to detect adhesion proteins and
226 vascular cell markers in adjacent sections: mouse-anti-human PECAM-1 antibody (CD31, clone
227 JC70A, Dako Agilent Technologies, Glostrup, Denmark) diluted 1:20 was used as a marker of
228 endothelial cells, rabbit-anti-human Tal1 (clone ab71333, Abcam, Cambridge, UK) diluted 1:80 was
229 used for talin-1, mouse-anti-human Tal2, (clone 68E7, Cancer Research Technology, London, UK)
230 diluted 1:100 was used for talin-2 and rabbit anti human Vin (clone ab61186, Abcam, Cambridge, UK)
231 diluted 1:50 was used vinculin. Samples were incubated with diluted primary antibodies at $+4^{\circ}\text{C}$
232 overnight, followed by washing 3 times with PBS. AlexaFluor-568 labeled goat-anti-mouse IgG (Cat #
233 A11004, Thermo Fisher Scientific) and AlexaFluor-488 labeled donkey-anti-rabbit IgG (Cat # A21206,
234 Thermo Fisher Scientific) antibodies diluted 1:100 were incubated on the samples for 1 hour at room
235 temperature to detect the bound primary antibodies. Immunostained samples were washed 5 times
236 with PBS, followed by one wash with deionized water. Glass coverslips were mounted on the samples
237 by using Prolong Diamond (Cat # P36962, Thermo Fisher Scientific) containing DAPI for nuclear
238 staining.

239 For immunofluorescence staining of formalin-fixed and paraffin-embedded (FFPE) samples, $4\ \mu\text{m}$
240 sections were cut from paraffin-embedded samples of LITA and healthy carotid artery and abdominal
241 aorta. Samples of LITA were collected from patients diagnosed with atherosclerosis, while the
242 samples of carotid artery and abdominal aorta were collected from a cadaver with no coronary artery
243 disease. Hematoxylin-eosin (HE) stained tissue sections were used to confirm normal tissue
244 morphology of these samples. All tissue sections were deparaffinized and rehydrated by incubating
245 them in xylene and in 99%, 95%, 70% and 50% ethanol solution for 10 min in each. For antigen
246 retrieval, tissue sections were boiled in 10 mM sodium citrate buffer (pH 6) with 0.05% Tween-20 for
247 20 min in a microwave oven and allowed to slowly cool back to room temperature. Samples were
248 washed 3 times with PBS (pH 7.4) and treated with 0.1% Sudan Black B for 20 min at room
249 temperature to quench tissue autofluorescence. Samples were washed 3 times 10 min with PBS and
250 immunostained using the same methods used for the frozen tissue sections. Antibody specificity was
251 confirmed by using control samples with no primary antibodies.

252 The immunolabeled sections were examined under a laser scanning confocal microscope (Zeiss Cell
253 Observer.Z1 equipped with a 63x/NA 1.4 oil immersion objective and Zeiss LSM780 confocal unit,
254 Carl Zeiss Microscopy, Jena, Germany). For fluorophore excitation, 480 nm argon laser and 405 nm
255 and 561 nm diode lasers were used together with suitable filter sets. For comparative analysis, the
256 laser intensities, PMT gains and other settings were kept constant for all samples. Serial plane images
257 were collected throughout the whole thickness of the sample at 200 nm intervals. During image
258 processing, maximum intensity projections were used to extract high intensity areas from the image
259 stacks into single images.

260

261 **Statistical Analyses**

262 Statistical analyses were performed using R version 2.15.0. To estimate fold changes between groups
263 in microarray analysis (MA), differences between medians (in \log_2 scale) were calculated. The \log
264 ratios were back-transformed to fold changes. To ease the interpretation, fold-change values <1 were

265 replaced by the negative of its inverse. Statistical significance of differences in gene expression was
 266 assessed using the nonparametric Wilcoxon signed-rank test and the log-transformed data. For
 267 associations between *TLN1*, *TLN2*, *meta-VCL* and *VCL* expression levels and SMC-rich
 268 plaque/macrophage markers, the Spearman correlation coefficient was used. To test the effect of
 269 covariates on expression levels of *TLN1*, *TLN2*, *meta-VCL* and *VCL*, Wilcoxon rank-sum test and
 270 Spearman correlation were used. The associations between covariates and expression levels were
 271 tested in the atherosclerotic plaque and LITA samples separately and were considered significant
 272 when $p < 0.05/42$ to 0.001 according to the Bonferroni correction for multiple testing. Differences were
 273 considered significant when $p < 0.05$.

274

275 Limitations of the study

276 Due to the poor availability of control arterial samples from healthy persons with no coronary artery
 277 disease, LITA samples obtained during coronary artery bypass surgery were used as controls for the
 278 studied plaque samples. LITA samples were collected from patients diagnosed with coronary artery
 279 disease. Therefore, the levels of talin-1, talin-2 and vinculin transcript expression profiles in LITA may
 280 not exactly match their expression profile in artery samples from healthy subjects with no diagnosed
 281 CAD. Therefore, immunostaining of talin-1 was used to confirm similar expression pattern of talin-1 in
 282 the LITA samples from CAD patients and in artery sample from healthy subject (Figure 4). In addition,
 283 similar artery morphology for these samples was confirmed by observing tissue sections with
 284 HE-staining (Figure 4). Another limitation of our study is the relatively small sample group size used.
 285 The small sample group size results from the poor availability of suitable patient samples and it was
 286 taken into consideration in the interpretation of the results.

287

288

289 Results

290 Characteristics of the subjects and studied samples

291 The demographics and risk factors of studied population are presented in Table 1. All internal arteries
 292 used as controls were verified microscopically as normal. Body mass index, occurrence of
 293 hypercholesterolemia, high blood pressure, coronary artery disease and history of myocardial
 294 infarction differed significantly between control group and group with atherosclerotic plaques. For
 295 mononuclear and whole blood analysis, patients with coronary artery disease considered as case
 296 group differed significantly in hypercholesterolemia occurrence, statin medication use and history of
 297 myocardial infarction from the control group. Because of these significant differences in the population,
 298 the gene expression was analyzed separately between these groups.

Table 1 Demographics and risk factors of the study patients included in the Tampere Vascular Study [10].

	Arterial Control	Plaque Case	Mononuclear/whole blood	
			CAD Control	CAD Case
No. of subjects	24	68	44	52
Age, y (median, SD)	69.0 (8.6)	70.0 (10.4)	57.0 (8.6)	56.5 (8.6)
Men (%)	82.1	67.6	63.0	61.5
Body mass index, kg/m ² (median, SD)	28.2 (5.1)	26.0 (4.0)*	27.7 (4.2)	26.9 (4.3)
History of smoking, %	64.3	75.0	53.3	65.4
Diabetes mellitus, %	32.1	23.5	8.7	19.2
Hypercholesterolemia, %	85.7	67.6*	52.2	76.9*
Hypertension, %	100.0	82.4*	84.8	96.2
Antihypertensive medication, %	92.9	80.9	80.4	92.3
Statin medication, %	82.1	73.5	20.4	73.1*

Coronary artery disease, %	100.0	29.4**	0.0	100.0***
Myocardial infarction, %	40.7	13.2*	23.9	57.7***

Pearson chi-square test and Wilcoxon signed-rank test was used for categorical and continuous risk factors, respectively. $p < 0.05$ *, $p < 0.01$ ** , $p < 0.001$ ***.

299 **Talin-1, talin-2 and vinculin transcripts are robustly expressed in left internal**
300 **thoracic artery (LITA) controls with significant reduction in plaques.**

301 The gene expression profiles of talin-1, talin-2 and vinculin were investigated to understand the
302 molecular mechanisms behind atherosclerosis. All three transcripts were robustly expressed in LITA
303 samples (Supplementary Table S1a) and in all plaque samples of the three analyzed arterial beds
304 (Supplementary Table S1b). Microarray analysis (MA) and low-density qRT-PCR (LDA) array showed
305 that all tested talin and vinculin transcripts were downregulated in atherosclerotic plaques ($fc < -1.6$,
306 for all plaques, with MA and LDA, $p < 0.00001$ (Supplementary Table S2, Figure 1a-d). In more detail,
307 all transcripts were downregulated in plaques of carotid, abdominal aortic and femoral arterial beds in
308 comparison to LITA (Supplementary Table S2, Figure 1e-h). The downregulation of talin-1 and talin-2
309 was most substantial in femoral plaques in comparison to LITA, whilst meta-vinculin was most
310 downregulated in carotid plaques and vinculin in abdominal aortic plaques in comparison to LITA.

311 [Figure 1]

312 **Expression of talin-1, talin-2 and vinculin transcripts is downregulated in both**
313 **stable and unstable atherosclerotic plaques**

314 We further characterized the expression profiles as a function of disease progression. According to
315 microarray analysis, all tested transcripts were downregulated in all plaques in comparison with LITA
316 controls (Supplementary Table S2, Figure 1a-d). Even though no significant reduction was observed
317 between the stable and unstable atherosclerotic plaque, a negative tendency in expression was seen
318 for talin-1, talin-2 and meta-vinculin between the stable and unstable plaques (Figure 1a-d).

319 **Talin-1 and vinculin transcripts are expressed in whole blood and circulating**
320 **monocytes.**

321 In order to evaluate if the expression profiles could be monitored using blood samples, whole blood
322 and circulating monocytes were analyzed. Talin-1, meta-vinculin and vinculin were robustly expressed
323 in whole blood samples while talin-2 was not detected in whole blood (Supplementary Table S1a). No
324 significant difference was observed between patients with history of coronary artery disease (CAD)
325 and controls in the whole blood expression levels of talin-1, talin-2, meta-vinculin and vinculin in MA
326 (fold change (fc) = $-1.01 - 1.03$, for all, $p > 0.3$) or in LDA analysis (fold change (fc) = $-1.13 - 1.05$, for
327 all, $p > 0.3$). Moreover, no significant differences were observed in the whole blood samples of the
328 patients with hypercholesterolemia, statin usage or patients with myocardial infarction. Expression in
329 circulating monocytes was statistically insignificant between controls and CAD patients for talin-1,
330 talin-2, meta-vinculin or vinculin transcripts. Nominally significantly reduced expression was however
331 observed for patients with myocardial infarction events for talin-1 ($fc = -1.13$, $p = 0.026$) and for
332 vinculin ($fc = -1.12$, $p = 0.03$) in circulating monocytes. However, no associations between gene
333 expression and clinical risk factors remained statistically significant after correcting for multiple testing.

334 **Hierarchical Clustering Analysis; association of talin-1, talin-2 and vinculin**
335 **transcripts with SMC and inflammation markers**

336 Hierarchical clustering based on the expression of the two inflammatory and two SMC markers
337 showed distinct separation of plaque samples from the LITA controls. Expression of talin-1, talin-2 and
338 vinculin was dependent on expression of SMC markers (*CNN1* and *SMTN*). Furthermore, high
339 expression of *TLN1*, *TLN2*, *VCL* and SMC markers with low expression of inflammatory biomarkers
340 *CD68* and *ALOX5* was observed in LITA controls (Figure 2). Also plaque samples of all tested arterial

341 beds separated into two distinct branches of the dendrogram. The samples exhibiting greater
342 reduction in *TLN1*, *TLN2* and *VCL* expression contained mainly carotid arterial samples, whereas
343 majority of femoral arterial beds showed smaller changes in the expression reduction.

344 [Figure 2]

345

346 **Talin-1, talin-2 and vinculin transcripts expression levels correlate with SMC-rich** 347 **atherosclerotic plaque signature**

348 To study the connection between gene expression and plaque composition, the expression profiles
349 were correlated with the known markers of smooth muscle cells (SMC). Utilizing markers of M1 and
350 M2 macrophages and SMC-rich plaque signature, we found that talin-1, talin-2 and both vinculin
351 transcripts correlate positively with SMC-rich plaque signature and in majority negatively with M1 and
352 M2 macrophage signatures (Supplementary Figure S1).

353

354 **Talin-1, talin-2 and vinculin localization in the atherosclerotic plaque cells** 355 **according to Confocal Immunofluorescence Analysis**

356 To get information about the protein localization within the blood vessel samples, immunofluorescence
357 staining of frozen tissue sections from atherosclerotic plaque and LITA controls were used to study
358 adhesion protein localization and expression in advanced disease. Talin-1 was found to be highly
359 expressed in the vascular endothelial cells of LITA samples (Figure 3a). On the contrary, talin-1
360 staining was not observed in the endothelial cells of an atherosclerotic artery. Furthermore, in the
361 thickened tunica intima (I) underlying the endothelial cells, gradual increase in talin-1 expression was
362 seen towards tunica media (M).

363 Antibody staining for talin-2 was observed to only partially colocalize with talin-1 staining in the tunica
364 intima (I) and tunica media (M) in LITA samples (Figure 3b). Interestingly, in tunica media of LITA
365 controls, talin-2 expression was higher in the luminal side and gradually decreased towards tunica
366 adventitia (A). In plaque samples, talin-2 expression in the endothelial cells was decreased, but not to
367 the same extent as talin-1 expression. In LITA samples, vinculin was found to be expressed in both
368 tunica intima (I) and tunica media (M), but not in tunica adventitia (A).

369 In tunica media, vinculin expression was higher close to the lumen and lower deeper inside the vessel
370 wall (Figure 3c). In plaque samples, decreased expression of vinculin in endothelial cells was
371 observed, but in the lower parts of the thickened intima vinculin was still expressed. As expected, the
372 expression of endothelial adhesion molecule PECAM-1 was found to be higher in the endothelium of
373 atherosclerotic plaques compared to the control samples from healthy arteries [32] (Figure 3a, c).

374 [Figure 3]

375

376 **Samples from LITA and healthy carotid artery and abdominal aorta show similar** 377 **tissue morphology and talin-1 expression patterns**

378 To confirm similar tissue morphology and talin-1 expression patterns in healthy carotid artery and
379 abdominal aorta and in the LITA samples used as a control in this study, tissue sections of
380 formalin-fixed and paraffin-embedded (FFPE) samples were stained with talin-1 antibody and
381 hematoxylin-eosin (HE) staining. Immunofluorescence staining of FFPE samples with talin-1 antibody
382 showed strong specific staining of talin-1 in tunica intima (I) and tunica media (M) in samples from
383 LITA and from healthy carotid artery and abdominal aorta (Figure 4). Similarly to the sections from
384 frozen LITA, the analyzed FFPE sections from LITA or healthy arteries showed uniform talin-1 staining

385 intensity, suggesting that the talin-1 gradient observed in plaque samples is unique feature. In
386 addition, HE staining of the FFPE samples showed similar tissue morphology for samples from LITA
387 and carotid artery and abdominal aorta (Figure 4). These experiments confirm the feasibility of using
388 LITA samples from CAD patients as negative controls for samples from atherosclerotic plaques when
389 studying expression patterns of focal adhesion proteins.

390

391 [Figure 4]

392

393 Discussion

394 In this study we show for the first time that the gene expression of talin-1, talin-2, meta-vinculin and
395 vinculin is significantly reduced in atherosclerotic plaques. Significant downregulation of expression
396 was observed in all of the studied carotid, abdominal aortic and femoral arterial beds compared to
397 LITA controls. However, expression of neither gene was changed in circulating monocytes or in whole
398 blood samples in CAD patients compared to controls.

399 We speculate that reduction in talin-1 expression in the endothelium may be one of the initial triggers
400 for the atherosclerotic plaque formation (Figure 5). Such downregulation could be caused by an
401 external factor such as altered shear stress and increased blood pressure. It has long been suspected
402 that the mechanosensing and mechanotransduction affects the DNA packing and may contribute to
403 changes in the protein expression in health and in disease [33] [34]. Another reason may lie in the
404 mutation affected control of gene expression levels leading to changes in the cell mechanobiology and
405 susceptibility to plaque development. In addition, recently the importance of miRNAs in the regulation
406 of gene expression in endothelial dysfunction has become evident, as discussed by Novák et al. [35].
407 Furthermore, one of the contributing factors of detected downregulation in this study may be the
408 changed cell composition in the advanced atherosclerotic plaque which can be seen on the confocal
409 images. Changes in acting mechanical force may also alter the signaling pathways related to focal
410 adhesions and affect the expression levels. In connection to atherosclerosis, the magnitude of shear
411 stress was shown to affect the expression of adhesion molecules facilitating endothelial cell-leukocyte
412 adhesion at the vascular lumen (vascular cell adhesion molecule (VCAM), intercellular cell adhesion
413 molecule (ICAM) or platelet endothelial cell adhesion molecule (PECAM) [36] [32]. Our previous
414 studies have also shown that the focal adhesions are compromised by reduced expression of integrin
415 family proteins and kindlin-2 in the endothelium and SMCs in the atherosclerotic plaque (*ITGA1*,
416 *ITGAV*, *ITGB1*, *ITGB3*, *ITGB5*, *FERMT2*), while the leukocyte adhesion is accelerated by increased
417 expression of leukocyte integrin-B2 and kindlin-3 [10]. The exact reasons for the observed reduction of
418 the talin and vinculin expression level remain, however, unclear and require attention in future studies.

419 [Figure 5]

420 Altered expression of talin-1, 2, meta-vinculin and vinculin may have severe impact on the cell's ability
421 to withstand varying magnitudes of acting mechanical forces, affect cell locomotion, cell/cell and cell-
422 ECM communication since both talin and vinculin are among the major constituents of the focal
423 adhesion complexes and are essential for cellular well-being [37]. Talin acts as molecular scaffolding
424 protein and may contribute to adhesion signaling via its binding partners, converting mechanical
425 signals to chemical cues [38]. Therefore, a reduction in talin-1 expression could render the
426 endothelium and the vascular wall prone to endothelial injury compared to mechanically stable
427 endothelial cell [39]. Endothelial injury triggers leukocyte adhesion and promotes inflammatory
428 response at the intima due to exposure of subendothelial collagen and other ECM components.
429 Confocal microscopy images of atherosclerotic plaque show increased PECAM-1 staining in the
430 intima, which points to increased leukocyte adhesion molecules and progression of inflammation at
431 the intima.

432 In addition, endothelium functions as a barrier for large molecules to enter the vessel wall and trigger
433 pathological processes in the inner vessel layers [40] [41]. In other words, the mechanostability of
434 endothelial cells including the endothelial intercellular gap and tight junction maintenance is crucial for
435 healthy vessel wall. Experiments with talin knockout cells show dramatically decreased capability of
436 cells to adhere, revealing the central role of talin in mediating the intracellular-extracellular connection.
437 The reduction in talin-1, talin-2, meta-vinculin and vinculin expression in the endothelium may affect
438 the ability of endothelial cells to adhere to each other and to ECM to form consistent blood-tissue
439 barrier. This could allow the inflammatory agents to progress into the tunica media and trigger
440 macrophage accumulation in the intima and media leading to arterial wall thickening and plaque
441 formation. Such effect can be observed in the presented tissue images where plaque staining shows
442 dramatically thickened intima layer with gross disorganization of the cells and low talin-1 and talin-2
443 intensity (reduced expression of talin-1 and talin-2 in plaque sample).

444 Studies by others have also shown the importance of talin-1 and talin-2 for cell, tissue and organ
445 development [42] [43]. Such importance of talin proteins on development was illustrated by talin-1
446 knockout experiments in HUVEC cells [44] [45] leading to severe phenotypes in mice embryos. The
447 phenotype is represented by abnormal vascular development affecting the growth of other major
448 tissues [45]. Furthermore, increased talin-1 expression has been detected in aggressive cancers as
449 well as in hypertrophic myocardium and failing heart [46] [47] [48]. Even though the downregulation of
450 neither talin-1 nor talin-2 has been to date directly linked to or associated with a disease, the reduced
451 expression may affect the vessel tissue formation, remodeling or healing and recovery. The confocal
452 images of the atherosclerotic plaque show gross disorganization of the cells in the vessel wall. Such
453 additional effects may lead into worsening of the site inflammation and progress of the disease to
454 severe, unstable atherosclerotic plaques. Even though the difference in expression between stable
455 and unstable atherosclerotic plaque reported here was not significant for the investigated transcripts,
456 negative tendency in expression levels was observed for talin-1, talin-2 and meta-vinculin. This
457 suggests that the expression of these genes is further reduced in the advanced disease.

458 The expression of talin-1 and talin-2 may also differ among the cells depending on the position in the
459 vessel wall layer. As can be seen in the talin-2 LITA staining, the intensity of talin-2 expression in
460 smooth muscle is higher in the layers closer to the intima where the mechanical impacts are expected
461 higher. Similar stratification has not been observed for talin-1 or vinculin in LITA controls. Whether
462 such stratification in healthy tissue is biologically and physiologically important remains open for
463 further investigation.

464

465 **Conclusion**

466 Talin-1, talin-2, meta-vinculin and vinculin expression is downregulated in atherosclerotic plaque.
467 Downregulation of expression was observed in plaques from all of the studied peripheral arterial beds
468 (carotid, abdominal aortic and femoral).

469 Even though the difference between stable and unstable atherosclerotic plaque was not significant for
470 the investigated transcripts, negative tendency was observed for talin-1, talin-2 and meta-vinculin. This
471 suggests that the expression of talins and vinculin is further reduced in the progression of the disease.

472 The central role of talin in cell adhesion proposes that the disintegration of the tissue in atherosclerosis
473 could be partially driven by downregulation of talin, leading to loosening of cell-ECM interactions and
474 reorganization of the tissue.

475 In conclusion we state that proteins contributing to mechanosensing, talin and vinculin, may have
476 important role in atherosclerotic plaque formation and disease progression.

477

478 **Acknowledgement and Funding Sources**

479 This work was supported by the Academy of Finland: grants 290506, 273192, 136288 (V.P.H),
480 286284 (T.L.), 285902 (E.R.), 134309; the Tampere University Hospital Medical Funds (grant X51001
481 (T.L), 9S054 (E.R) and X51410 (V.P.H)); the Finnish Foundation of Cardiovascular Research (T.L.);
482 the Finnish Cultural Foundation (R.R.); the Tampere Tuberculosis Foundation (T.L. and N.O.); the
483 Emil Aaltonen Foundation (T.L. and N.O.); and the Yrjö Jahnsso Foundation (T.L. and N.O.). This
484 work was also supported by the European Union 7th Framework Programme funding for the
485 AtheroRemo project [201668] and Fimlab Laboratories. We thank the University of Tampere for
486 financial support via the TGPBB graduate school (M.v.E.).

487

488 **Figure Legends**

489

490 Figure 1 Expression of talin (*TLN*) and vinculin (*VCL*) transcripts. Results of Microarray Analysis (MA).
491 (a-d) Expression levels in LITA controls and all, stable and unstable atherosclerotic plaques. (e-f)
492 Expression levels in carotid, abdominal aortic and femoral arterial bed compared to LITA controls.

Figure 2 Heat maps of log₂ expression values. Talin-1 (*TLN1*), Talin-2 (*TLN2*) and vinculin (*VCL*) co-expression with biomarkers of inflammation (*CD68*, *ALOX5*) and smooth muscle cells markers (*CNN1*, *SMTN*). The expression values of each row (gene) are scaled to z-scores, color-code for expression values and arterial site is presented in the top-right corner. The dendrogram illustrates hierarchical clustering based on the seven robustly expressed genes. The top bar represents the arterial site origin of the sample tissue.

Figure 3 Tissue localization of talin-1, talin-2 and vinculin in atherosclerotic plaque from carotid artery and left internal thoracic (LITA) control. (a) talin-1 and PECAM-1, (b) talin-1 and talin-2, (c) vinculin and PECAM-1. Talin-1 was expressed in the endothelial cells of LITA, while talin-1 expression in plaque endothelial cells was not observed (a). Talin-2 expression was decreased in plaque endothelium as compared to LITA, but not as strongly as talin-1 expression (b). In LITA, high vinculin expression was observed in tunica intima and at the luminal side of tunica media. In plaque samples, decreased vinculin expression was observed in the thickened tunica intima (c). PECAM-1 expression was found to be increased in plaque endothelium (a, c). L: lumen, I: tunica intima, E1: internal elastic lamina, E2: external elastic lamina, M: tunica media, A: tunica adventitia.

Figure 4 Tissue morphology and localization of talin-1 in immunostained FFPE sections of LITA from patients with coronary artery disease and healthy abdominal aorta and carotid artery. Uniform talin-1 immunostaining was observed in tunica intima and tunica media in both immunostained LITA samples, as well as in the samples from healthy abdominal aorta and carotid artery. HE-staining showed normal tissue morphology for all of the analyzed samples. In the merged images, talin-1 immunostaining is shown as green and DAPI chromatin staining as blue. L: lumen, I: tunica intima, E1: internal elastic lamina, E2: external elastic lamina, M: tunica media, A: tunica adventitia.

Figure 5 Simplified speculative model for downregulation of talin expression in vascular endothelium as initial trigger of atherosclerotic plaque formation.

493 References

494

- 495 [1] A. S. Antonov, F. D. Kolodgie, D. H. Munn, and R. G. Gerrity, "Regulation of macrophage
496 foam cell formation by alphaVbeta3 integrin: potential role in human atherosclerosis.," *Am. J.*
497 *Pathol.*, 2004.
- 498 [2] P. F. Davies, "Flow-mediated endothelial mechanotransduction.," *Physiol. Rev.*, 1995.
- 499 [3] W. C. Aird, "Endothelial cell heterogeneity," *Cold Spring Harb. Perspect. Med.*, 2012.
- 500 [4] W. C. Aird, "Spatial and temporal dynamics of the endothelium," *J Thromb Haemost*, vol. 3, pp.
501 1392–1406, 2005.
- 502 [5] J. P. Califano and C. A. Reinhart-King, "Exogenous and endogenous force regulation of
503 endothelial cell behavior," *J. Biomech.*, 2010.
- 504 [6] J. F. Keaney, "Atherosclerosis: From lesion formation to plaque activation and endothelial
505 dysfunction," *Mol. Aspects Med.*, 2000.
- 506 [7] T. J. Chancellor, J. Lee, C. K. Thodeti, and T. Lele, "Actomyosin tension exerted on the
507 nucleus through nesprin-1 connections influences endothelial cell adhesion, migration, and
508 cyclic strain-induced reorientation," *Biophys. J.*, 2010.
- 509 [8] Z. Jahed, H. Shams, M. Mehrbod, and M. R. K. Mofrad, "Mechanotransduction pathways
510 linking the extracellular matrix to the nucleus," *Int. Rev. Cell Mol. Biol.*, 2014.
- 511 [9] N. Oksala, M. Levula, N. Airla, M. Pelto-Huikko, R. M. Ortiz, O. Järvinen, J.-P. Salenius, B.
512 Ozsait, E. Komurcu-Bayrak, N. Erginel-Unaltuna, A.-P. J. Huovila, L. Kytömäki, J. T. Soini, M.
513 Kähönen, P. J. Karhunen, R. Laaksonen, and T. Lehtimäki, "ADAM-9, ADAM-15, and ADAM-
514 17 are upregulated in macrophages in advanced human atherosclerotic plaques in aorta and
515 carotid and femoral arteries--Tampere vascular study.," *Ann. Med.*, 2009.
- 516 [10] N. Oksala, J. Pärssinen, I. Seppälä, N. Klopp, T. Illig, R. Laaksonen, M. Levula, E. Raitoharju, I.
517 Kholova, T. Sioris, M. Kähönen, T. Lehtimäki, and V. P. Hytönen, "Kindlin 3 (FERMT3) is
518 associated with unstable atherosclerotic plaques, anti-inflammatory type II macrophages and
519 upregulation of beta-2 integrins in all major arterial beds," *Atherosclerosis*, vol. 242, no. 1, pp.
520 145–154, 2015.
- 521 [11] J. Winkler, H. Lünsdorf, and B. M. Jockusch, "Energy-filtered electron microscopy reveals that
522 talin is a highly flexible protein composed of a series of globular domains.," *Eur. J. Biochem.*,
523 1997.
- 524 [12] A. R. Gingras, W. H. Ziegler, A. A. Bobkov, M. G. Joyce, D. Fasci, M. Himmel, S. Rothemund,
525 A. Ritter, J. G. Grossmann, B. Patel, N. Bate, B. T. Goult, J. Emsley, I. L. Barsukov, G. C. K.

- 526 Roberts, R. C. Liddington, M. H. Ginsberg, and D. R. Critchley, "Structural determinants of
527 integrin binding to the talin rod," *J. Biol. Chem.*, 2009.
- 528 [13] A. R. Gingras, N. Bate, B. T. Goult, L. Hazelwood, I. Canestrelli, J. Gü Nter Grossmann, H. Liu,
529 N. Sm Putz, G. C. Roberts, N. Volkmann, D. Hanein, I. L. Barsukov, and D. R. Critchley, "The
530 structure of the C-terminal actin-binding domain of talin," *EMBO J.*, vol. 27, pp. 458–469, 2008.
- 531 [14] B. T. Goult, A. R. Gingras, N. Bate, I. L. Barsukov, D. R. Critchley, and G. C. K. Roberts, "The
532 domain structure of talin: Residues 1815-1973 form a five-helix bundle containing a cryptic
533 vinculin-binding site," *FEBS Lett.*, 2010.
- 534 [15] E. Papagrigoriou, A. R. Gingras, I. L. Barsukov, N. Bate, I. J. Fillingham, B. Patel, R. Frank, W.
535 H. Ziegler, G. C. Roberts, D. R. Critchley, and J. Emsley, "Activation of a vinculin-binding site
536 in the talin rod involves rearrangement of a five-helix bundle," *EMBO J.*, vol. 23, pp. 2942–
537 2951, 2004.
- 538 [16] V. P. Hytönen and V. Vogel, "How force might activate talin's vinculin binding sites: SMD
539 reveals a structural mechanism," *PLoS Comput. Biol.*, 2008.
- 540 [17] A. del Rio, R. Perez-Jimenez, R. Liu, P. Roca-Cusachs, J. M. Fernandez, and M. P. Sheetz,
541 "Stretching single talin rod molecules activates vinculin binding.," *Science*, 2009.
- 542 [18] B. T. Goult, T. Zacharchenko, N. Bate, R. Tsang, F. Hey, A. R. Gingras, P. R. Elliott, G. C. K.
543 Roberts, C. Ballestrem, D. R. Critchley, and I. L. Barsukov, "RIAM and vinculin binding to talin
544 are mutually exclusive and regulate adhesion assembly and turnover," *J. Biol. Chem.*, 2013.
- 545 [19] G. Di Paolo, L. Pellegrini, K. Letinic, G. Cestra, R. Zoncu, S. Voronov, S. Chang, J. Guo, M. R.
546 Wenk, and P. De Camilli, "Recruitment and regulation of phosphatidylinositol phosphate kinase
547 type 1 gamma by the FERM domain of talin.," *Nature*, 2002.
- 548 [20] G. Luo, A. H. Herrera, and R. Horowitz, "Molecular interactions of N-RAP, a nebulin-related
549 protein of striated muscle myotendon junctions and intercalated disks," *Biochemistry*, 1999.
- 550 [21] N. Sun, D. R. Critchley, D. Paulin, Z. Li, and R. M. Robson, "Identification of a repeated
551 domain within mammalian alpha-synemin that interacts directly with talin," *Exp. Cell Res.*,
552 2008.
- 553 [22] R. A. Borgon, C. Vonrhein, G. Bricogne, P. R. J. Bois, and T. Izard, "Crystal structure of human
554 vinculin.," *Structure*, 2004.
- 555 [23] S. Hüttelmaier, P. Bubeck, M. Rüdiger, and B. M. Jockusch, "Characterization of two F-actin-
556 binding and oligomerization sites in the cell-contact protein vinculin.," *Eur. J. Biochem.*, 1997.
- 557 [24] C. K. Wood, C. E. Turner, P. Jackson, and D. R. Critchley, "Characterisation of the paxillin-
558 binding site and the C-terminal focal adhesion targeting sequence in vinculin.," *J. Cell Sci.*,

- 559 1994.
- 560 [25] M. Kroemker, A. H. Rüdiger, B. M. Jockusch, and M. Rüdiger, “Intramolecular interactions in
561 vinculin control alpha-actinin binding to the vinculin head.,” *FEBS Lett.*, 1994.
- 562 [26] N. Oksala, J. Pärssinen, I. Seppälä, E. Raitoharju, K. Ivana, J. Hernesniemi, L. P. Lyytikäinen,
563 M. Levula, K. M. Mäkelä, T. Sioris, M. Kähönen, R. Laaksonen, V. Hytönen, and T. Lehtimäki,
564 “Association of neuroimmune guidance cue netrin-1 and its chemorepulsive receptor UNC5B
565 with atherosclerotic plaque expression signatures and stability in human(s) Tampere Vascular
566 Study (TVS),” *Circ. Cardiovasc. Genet.*, 2013.
- 567 [27] H. C. Stary, A. B. Chandler, S. Glagov, J. R. Guyton, W. Insull, M. E. Rosenfeld, S. A. Schaffer,
568 C. J. Schwartz, W. D. Wagner, and R. W. Wissler, “A definition of initial, fatty streak, and
569 intermediate lesions of atherosclerosis. A report from the Committee on Vascular Lesions of the
570 Council on Arteriosclerosis, American Heart Association.,” *Circulation*, 1994.
- 571 [28] T. Nieminen, R. Lehtinen, J. Viik, T. Lehtimäki, K. Niemelä, K. Nikus, M. Niemi, J. Kallio, T.
572 Kööbi, V. Turjanmaa, and M. Kähönen, “The Finnish Cardiovascular Study (FINCAVAS):
573 characterising patients with high risk of cardiovascular morbidity and mortality.,” *BMC*
574 *Cardiovasc. Disord.*, 2006.
- 575 [29] H. Turpeinen, I. Seppälä, L.-P. Lyytikäinen, E. Raitoharju, N. Hutri-Kähönen, M. Levula, N.
576 Oksala, M. Waldenberger, N. Klopp, T. Illig, N. Mononen, R. Laaksonen, O. Raitakari, M.
577 Kähönen, T. Lehtimäki, and M. Pesu, “A genome-wide expression quantitative trait loci analysis
578 of proprotein convertase subtilisin/kexin enzymes identifies a novel regulatory gene variant for
579 FURIN expression and blood pressure,” *Hum. Genet.*, vol. 134, no. 6, pp. 627–636, 2015.
- 580 [30] E. Raitoharju, I. Seppälä, L. P. Lyytikäinen, M. Levula, N. Oksala, N. Klopp, T. Illig, R.
581 Laaksonen, M. Kähönen, and T. Lehtimäki, “A comparison of the accuracy of Illumina
582 HumanHT-12 v3 Expression BeadChip and TaqMan qRT-PCR gene expression results in
583 patient samples from the Tampere Vascular Study,” *Atherosclerosis*, 2013.
- 584 [31] O. Puig, J. Yuan, S. Stepaniants, R. Zieba, E. Zycband, M. Morris, S. Coulter, X. Yu, J. Menke,
585 J. Woods, F. Chen, D. R. Ramey, X. He, E. A. O’Neill, E. Hailman, D. G. Johns, B. K. Hubbard,
586 P. Y. Lum, S. D. Wright, M. M. DeSouza, A. Plump, and V. Reiser, “A gene expression
587 signature that classifies human atherosclerotic plaque by relative inflammation status,” *Circ.*
588 *Cardiovasc. Genet.*, vol. 4, no. 6, pp. 595–604, 2011.
- 589 [32] E. Galkina and K. Ley, “Vascular adhesion molecules in atherosclerosis,” *Arteriosclerosis,*
590 *Thrombosis, and Vascular Biology*. 2007.
- 591 [33] E. K. Yim and M. P. Sheetz, “Force-dependent cell signaling in stem cell differentiation,” *Stem*
592 *Cell Research & Therapy*. 2012.

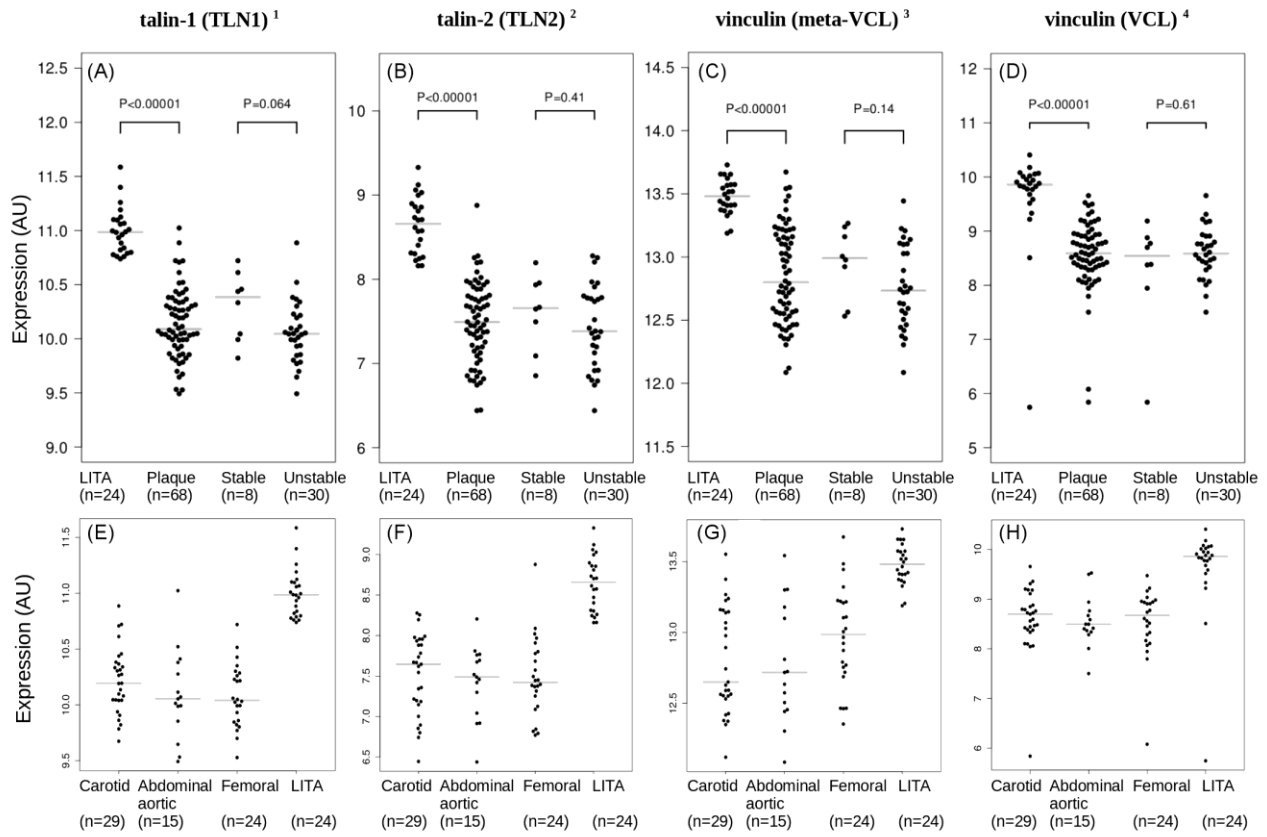
- 593 [34] M. Zwerger, C. Y. Ho, and J. Lammerding, “Nuclear mechanics in disease,” *Annu Rev Biomed*
594 *Eng*, 2011.
- 595 [35] J. Novák, V. Olejníčková, N. Tkáčová, and G. Santulli, “Mechanistic role of microRNAs in
596 coupling lipid metabolism and atherosclerosis,” *Adv. Exp. Med. Biol.*, vol. 887, pp. 79-100,
597 2015.
- 598 [36] T. Nagel, N. Resnick, W. J. Atkinson, C. F. Dewey, and M. A. Gimbrone, “Shear stress
599 selectively upregulates intercellular adhesion molecule-1 expression in cultured human vascular
600 endothelial cells,” *J. Clin. Invest.*, 1994.
- 601 [37] K. Austen, P. Ringer, A. Mehlich, A. Chrostek-Grashoff, C. Kluger, C. Klingner, B. Sabass, R.
602 Zent, M. Rief, and C. Grashoff, “Extracellular rigidity sensing by talin isoform-specific
603 mechanical linkages,” *Nat. Cell Biol.*, vol. 17, no. 12, pp. 1597–1606, 2015.
- 604 [38] V. P. Hytönen and B. Wehrle-Haller, “Protein conformation as a regulator of cell-matrix
605 adhesion,” *Phys. Chem. Chem. Phys.*, vol. 16, no. 14, pp. 6342–57, 2014.
- 606 [39] P. F. Davies, “Hemodynamic shear stress and the endothelium in cardiovascular
607 pathophysiology,” *Nat. Clin. Pract. Cardiovasc. Med.*, 2009.
- 608 [40] G. Satha, S. B. Lindström, A. Klarbring, G. Satha, S. B. Lindström, . A. Klarbring, and A.
609 Klarbring, “A goal function approach to remodeling of arteries uncovers mechanisms for growth
610 instability,” *Biomech Model Mechanobiol*, vol. 13, pp. 1243–1259, 2014.
- 611 [41] J. M. Tarbell, “Shear stress and the endothelial transport barrier,” *Cardiovascular Research*.
612 2010.
- 613 [42] S. J. Monkley, X. H. Zhou, S. J. Kinston, S. M. Giblett, L. Hemmings, H. Priddle, J. E. Brown,
614 C. A. Pritchard, D. R. Critchley, and R. Fässler, “Disruption of the talin gene arrests mouse
615 development at the gastrulation stage,” *Dev. Dyn.*, 2000.
- 616 [43] F. J. Conti, S. J. Monkley, M. R. Wood, D. R. Critchley, and U. Müller, “Talin 1 and 2 are
617 required for myoblast fusion, sarcomere assembly and the maintenance of myotendinous
618 junctions,” *Development*, 2009.
- 619 [44] P. M. Kopp, N. Bate, T. M. Hansen, N. P. J. Brindle, U. Praekelt, E. Debrand, S. Coleman, D.
620 Mazzeo, B. T. Goult, A. R. Gingras, C. A. Pritchard, D. R. Critchley, and S. J. Monkley,
621 “Studies on the morphology and spreading of human endothelial cells define key inter- and
622 intramolecular interactions for talin1,” *Eur. J. Cell Biol.*, 2010.
- 623 [45] S. J. Monkley, V. Kostourou, L. Spence, B. Petrich, S. Coleman, M. H. Ginsberg, C. A.
624 Pritchard, and D. R. Critchley, “Endothelial cell talin1 is essential for embryonic angiogenesis,”
625 *Dev. Biol.*, 2011.
- 626 [46] S. Sakamoto, R. O. McCann, R. Dhir, and N. Kyprianou, “Talin1 promotes tumor invasion and

627 metastasis via focal adhesion signaling and anoikis resistance,” *Cancer Res.*, vol. 70, no. 5, pp.
628 1885–1895, 2010.

629 [47] K. Fang, W. Dai, Y.-H. Ren, Y.-C. Xu, S. Zhang, and Y.-B. Qian, “Both Talin-1 and Talin-2
630 correlate with malignancy potential of the human hepatocellular carcinoma MHCC-97 L cell,”
631 *BMC Cancer*, vol. 16, no. 1, p. 45, 2016.

632 [48] A. M. Manso, R. Li, S. J. Monkley, N. M. Cruz, S. Ong, D. H. Lao, Y. E. Koshman, Y. Gu, K.
633 L. Peterson, J. Chen, E. D. Abel, A. M. Samarel, D. R. Critchley, and R. S. Ross, “Talin 1 has
634 unique expression versus talin 2 in the heart and modifies the hypertrophic response to pressure
635 overload,” *J. Biol. Chem.*, vol. 288, no. 6, pp. 4252–4264, 2013.

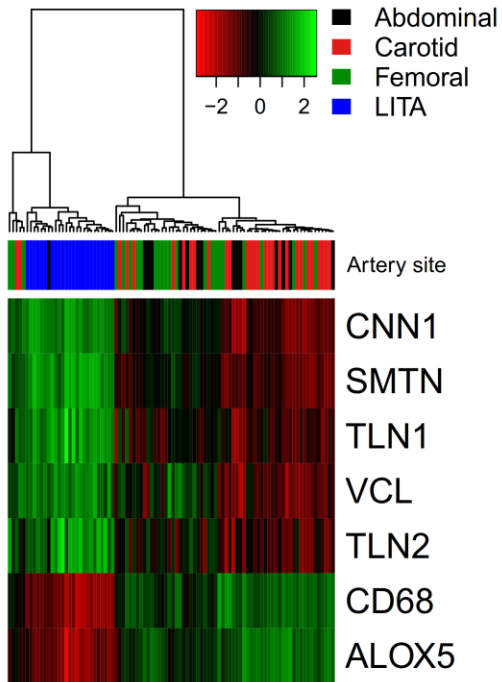
636
637
638
639
640
641
642
643
644
645
646
647
648
649
650
651
652
653
654
655
656
657
658
659
660
661
662
663
664



¹ ILMN_1696643, ² ILMN_1700042, ³ ILMN_1795429, ⁴ ILMN_2413527

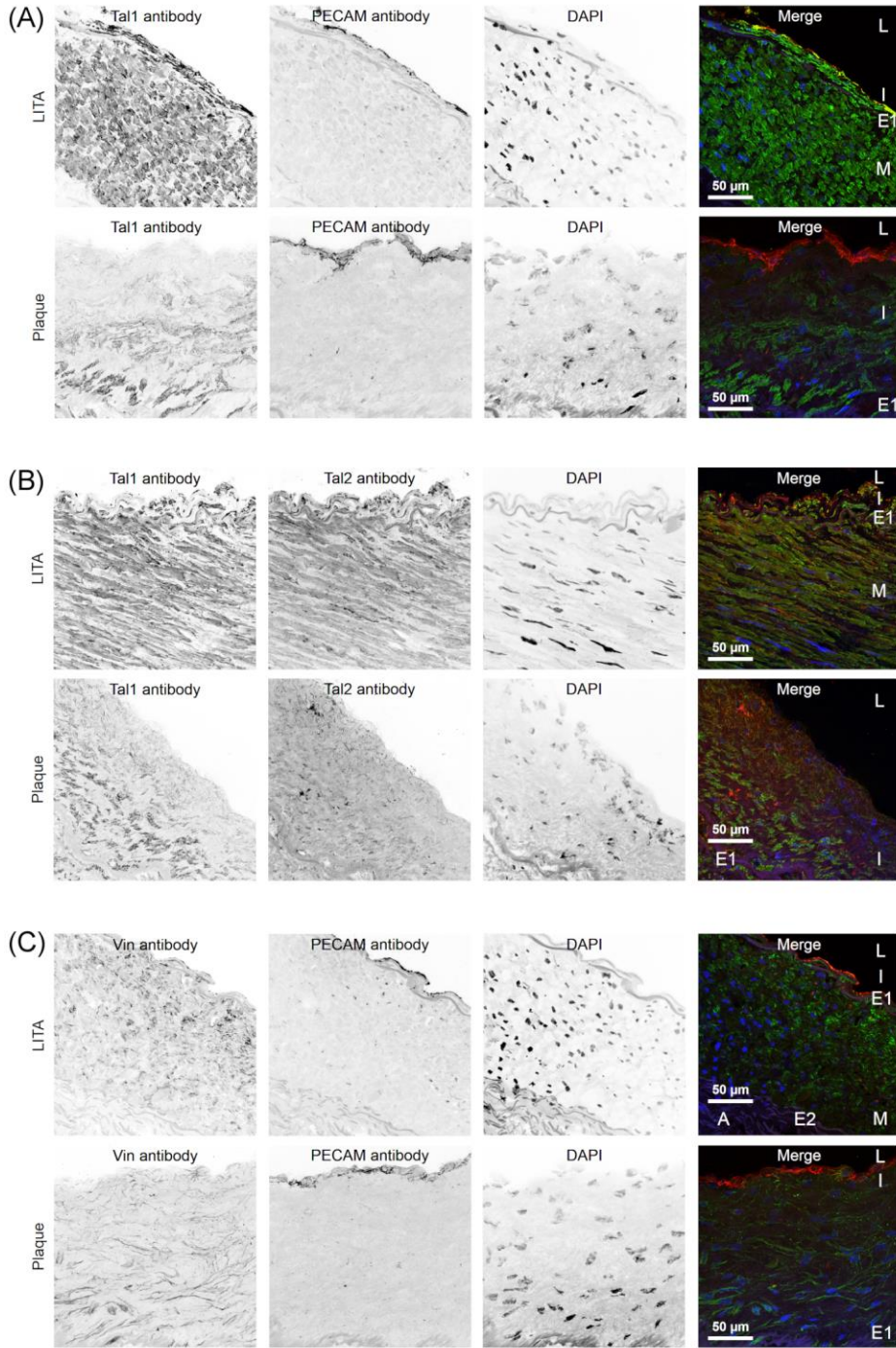
666
 667
 668
 669
 670
 671
 672
 673
 674
 675
 676
 677
 678
 679
 680
 681
 682

683 Fig. 2



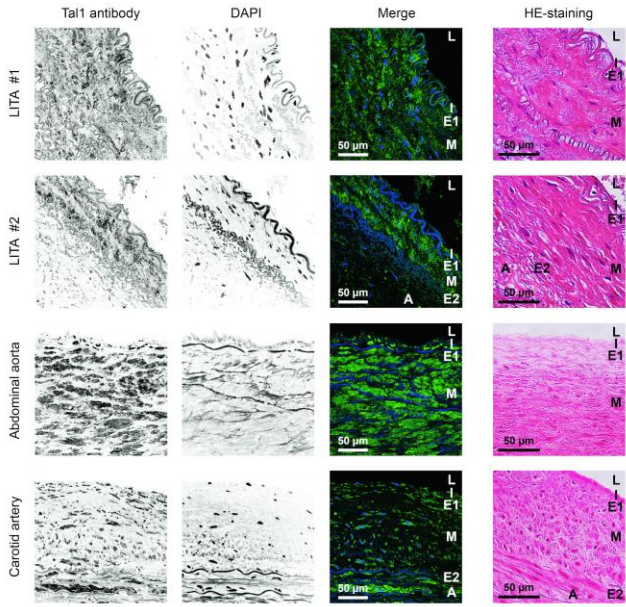
684
685
686
687
688
689
690
691
692
693
694
695
696
697
698
699
700
701
702
703
704
705
706

707 Fig. 3
708



709
710
711
712
713
714

715 Fig. 4



716
717
718
719
720
721
722
723
724
725
726
727
728
729
730
731
732
733
734
735
736
737
738
739

